Desalination and Water Treatment
www.deswater.com

doi: 10.1080/19443994.2014.936513

56 (2015) 399–408
October

Taylor & Francis
Taylor & Francis Group

Application of radial basis function neural network for removal of copper using an emulsion liquid membrane process assisted by ultrasound

Nabil Messikh[a], Mahdi Chiha[a,b,*], Fatiha Ahmedchekkat[a,b], Abeer Al Bsoul[c]

[a]*Faculty of Technology, Department of Petrochemical and Process Engineering, University of 20 Août 1955- Skikda, P.O. Box 26, 21000 Skikda, Algeria, Tel. +213 0 559089568; emails: nabchem@yahoo.fr (N. Messikh), ahmedchekkatf@yahoo.fr (F. Ahmedchekkat)*
[b]*Faculty of Technology, Environmental and Chemical Engineering Laboratory, University of 20 Août 1955- Skikda, P.O. Box 26, 21000 Skikda, Algeria, Tel. +213 0 0697727414; email: chiha_m_f@yahoo.fr*
[c]*Department of Chemical Engineering, Al-Huson University College, Al-Balqa Applied University, P.O. Box 50, Al-Huson, Irbid, Jordan, Tel. +0962775609706; email: abeer@yahoo.com*

Received 22 August 2013; Accepted 12 June 2014

ABSTRACT

In this present work, artificial neural network was applied for the prediction of the breakage percentage and the extraction efficiency for the removal of copper using emulsion liquid membrane process. The effect of operational parameters such as emulsification time, ultrasonic power, stirring speed, sulfuric acid concentration, extractant concentration, surfactant concentration, internal phase/organic phase volume ratio, emulsion/external phase volume ratio, and copper concentration in the external phase were studied to optimize the condition for maximum copper removal. The performance of the proposed model (radial basis function—RBF) for predicting copper removal efficiency was found to be very impressive. The RBF model perfectly represents the experimental data.

Keywords: Emulsion liquid membrane; Copper extraction; Artificial neural network; Radial basis function; Ultrasound

1. Introduction

Emulsion liquid membrane (ELM) extraction process, proposed by Li [1] constitutes a promising technology with a considerable potential for various applications, such as removal, recovery, and purification of pollutants from wastewater [2–5]. ELM has been used as an alternative to conventional liquid–liquid extraction processes. It has shown some advantages as they are rapid extraction process with a high efficiency (due to the large surface area available for mass transfer). Furthermore, it offers simultaneous extraction and stripping in a single step [6,7]. ELM is a three phase dispersion system, where a primary emulsion dispersed in a continuous phase, which is the phase to be treated. The liquid membrane separates the external continuous phase from the encapsulated phase. The solutes transported through the membrane from external phase and concentrated in the internal phase as droplets [7–9].

As any technique, ELM exhibits some drawbacks, such as membrane rupture, swelling, and membrane instability [10]. In order to overcome these problems arising in ELM, the applicability of artificial neural networks (ANN) was explored, a method inspired by the human brain, to predict the stability of emulsified

*Corresponding author.

W/O and the extraction efficiency of copper. A great advantage of ANN models is that it is not necessary to know the mathematical relationship between the input and output variables. Instead, it figures out these relationships through successive trainings [11]. ANN has a vast range of applications in the fields of agriculture, weather forecasting, finance and economics, medicine, robotics, material science, industrial chemistry, and chemical engineering, etc. [11–13].

ANN is a mathematical model based on biological neural networks. The basic element in ANN is the neuron (node). Fig. 1 shows a single neuron of ANN. Neurons are linked to each other by connections recognized as synapses, associated with each synapse there is a weight factor. These synaptic weights, multiply (amplify or attenuate) the input information [14,15]. Each of these units is a simplified model of a neuron and transforms its input into an output response. The transformation involves two steps: first, the activation of the neuron is computed as a weighted sum of its inputs, and second, this activation is transformed in response by using a transfer function. Generally, if each input is represented by x_i and each weight by w_i, then each input is multiplied by its corresponding weight factor and the neuron uses summation of these weighted inputs to approximate an output signal via a transfer function. Any function whose domain is a real number can be used as a transfer function. The most popular types of transfer functions are as follows: linear, step, threshold, and logarithmic sigmoid and hyperbolic tangent sigmoid functions.

A number of considerations must be taken into account when designing ANN model. First, the appropriate structure of ANN model must be chosen. Second, the activation function needs to be determined. The number of layers and the number of units in each layer must be chosen. Generally, desired models consist of a number of layers. The most general model assumes complete interconnections between all units. These connections can be bidirectional or unidirectional. ANN can create its own representation of the information it receives during learning time [15].

There are many types of ANNs such as back propagation neural network, a multilayer perceptron, and radial basis function (RBF) neural networks. Among them, RBF is a feed-forward and local adjustment network. Therefore, its training rate is faster than other neural networks. The training procedure is also simple because there are fewer parameters that have to be optimized: the width of the RBF and the number of units in the hidden layer [16].

The aim of this work was to predict the emulsion stability and the efficient extraction of copper by using RBF model. The efficiency of copper extraction was investigated at different conditions, such as emulsification time, ultrasonic power, stirring speed, sulfuric acid concentration, extractant concentration, surfactant concentration, internal phase/organic phase volume ratio, emulsion/external phase volume ratio, and concentration of copper in external phase. The RBF results were compared with those obtained through experiments.

2. Experimental

2.1. Chemical

Bis (2-ethylhexyl) phosphoric acid (D2EHPA) used was an analytical grade product (Aldrich). The nonionic surfactant Span80 (sorbitan monooleate, Aldrich) was used as an emulsifier. Diluents hexane was obtained from Fluka. Copper (II) solutions were prepared by dissolving a requisite amount of copper sulfate ($CuSO_4{\cdot}5H_2O$, Prolab) in distilled water. Analytically pure sulfuric acid, obtained from Merck, was employed in the preparation of the aqueous internal phase.

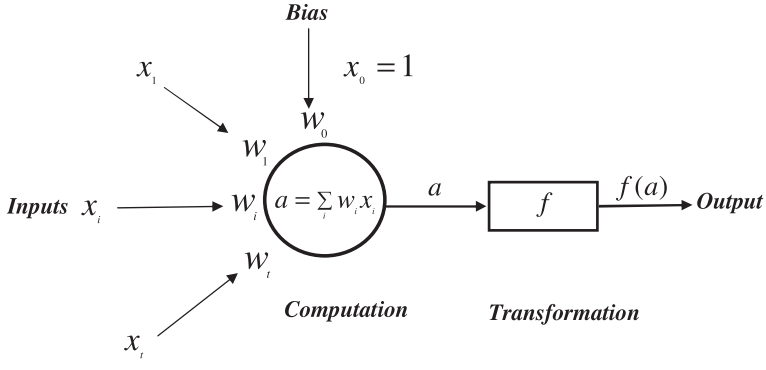

Fig. 1. Basic neural unit.

2.2. Apparatus and procedure

ELM was formed by mixing a requisite volume of the organic phase containing the (D2EHPA) with Span 80 as a surfactant in n-hexane as a diluent. Internal aqueous phase were prepared by dissolving the required amount of the appropriate sulfuric acid solution (H_2SO_4), in deionized water. The emulsion was formed by adding together the internal phase slowly to the organic membrane phase upon intensive emulsification by means of ultrasonics probe with an operating frequency of 22 kHz (Microson 200XL).

A certain volume of the stable emulsion obtained (20 mL) was dispersed in the feed phase (100 mL of aqueous solution). The extraction runs were performed in a glass vessel of 61 mm diameter using a mechanical agitator (Junke & Kunkel RW20) equipped with a four paddle impeller of 20 mm diameter. All experiments were carried out in a water vessel at a regulated temperature of 25 ± 1˚C. The concentration of copper in the aqueous external phase was determined by atomic absorption spectrophotometer (AAS, Shimadzu A. A-6601 F, Atomic Absorption Flame Emission Spectrophotometer) at 325 nm. The copper concentration in the internal phase was determined by mass balance.

2.3. Artificial neural network for prediction of experimental results

Neural network modeling is a nonlinear statistical technique. It can be used to model a complex relationship between the inputs and the outputs or to find patterns in data-sets. RBF network, the model proposed in this work, is the feed-forward neural network type, which is composed of three layers with entirely different roles. The input layer is made of source nodes that connect the network to its environment. The second layer is the hidden layer which applies a nonlinear transformation from the input space to the hidden space, which is of high dimensionality. The output layer is linear, supplying the response of the network to the activation patterns applied to the input layer [17]. Fig. 2 shows the general architecture of the RBF network.

In RBF networks, the determination of the number of neurons in the hidden layer is very important because of the general capability and the complexity of the network. If the number of the neurons in the hidden layer is insufficient, the RBF network cannot learn the data adequately; on the other hand, if the neuron number is too high, poor generalization or over learning may occur [18]. The outputs of the input layer are determined by calculating the distance between the network inputs and the hidden layer centers. The second layer is the linear hidden layer and the outputs of this layer are the weighted form of the input layer output. Each neuron of the hidden layer has a parameter vector called center. Therefore, a general expression of the network can be given as:

$$y_j = \sum_{i=1}^{I} w_{ij}\phi\left(||X - c_i||\right) + \beta_j \quad (1)$$

where ij: number of neurons in the hidden layer and the output layer, w_{ij}: weight of ith neuron and jth output, ϕ: RBF, x: Input data vector, C_i: center vector of ith neuron, β_j: bias value of the output jth neuron, y_j: network output of the jth neuron.

Training is an optimization procedure in which the network weights are adjusted in order to minimize the selected error value. The training procedure of RBF network determines the number of the hidden neurons required for the simulation. In this study, the root mean square error (RMSE) function was used to estimate the performance of the neural network:

$$RMSE = \sqrt{\frac{1}{n}\sum_{i=1}^{n}\left(y_{io} - y_i\right)^2} \quad (2)$$

where y_{io} is the target output value, y_i is the neural network output, and n is the total number of data patterns used.

3. Results and discussion

3.1. Emulsion stability

The experimental data were used to train the neural network. In the present study, the parameters which affect the emulsion stability were used as input variables of ANN model. The percentage volume of the internal phase leaked into the external phase as the output parameter of ANN model was considered as a measure of the emulsion breakage (Table 1).

The stability of emulsion (W/O) was investigated by using the breakup (ε), defined by the following equation:

$$\varepsilon = \frac{V_s}{V_{int}} \times 100 \quad (3)$$

The emulsion breakage represents the percentage ratio of the volume of the internal phase leaked into the external phase by splitting (V_s) to the initial volume of

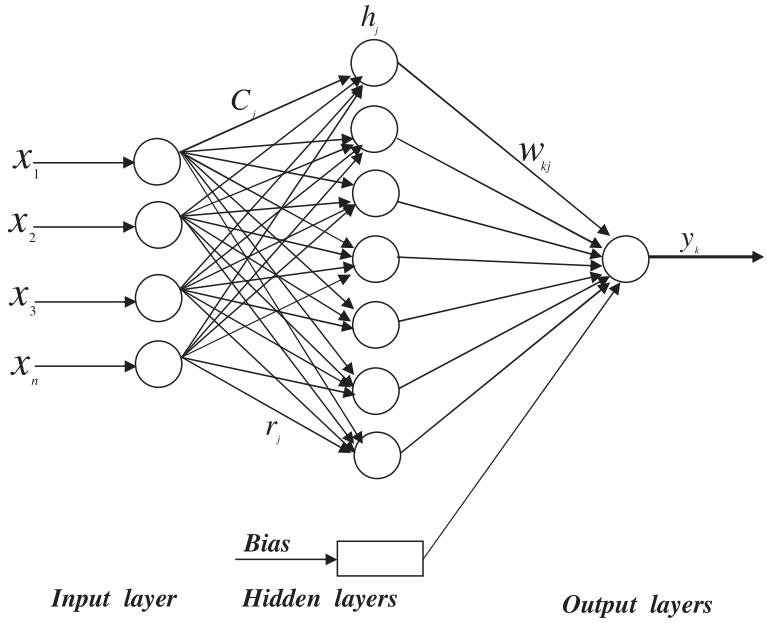

Fig. 2. The general architecture of RBF network.

Table 1
Ranges of input variable models

	Input variable	Symbol	Range
Stability of membrane	Emulsification time (min)	t_{em}	1–10
	Ultrasonic power (W)	P	10–35
	Stirring speed (rpm)	SS	100–500
	Sulfuric acid concentration (M)	[H_2SO_4]	0.1–1.2
	Extractant concentration (% (v/v))	[D2EHPA]	5–40
	Surfactant concentration (% (v/v))	[Span80]	2–8
	Volume ratio of internal phase to organic phase	V_{in}/V_{org}	0.5–2
Extraction of copper	Volume ratio of emulsion to external phase	V_{em}/V_{ext}	0.05–2
	Concentration of copper (ppm)	[Cu^{+2}]	50–200
	Contact time (min)	t	0.5–18
	Extractant concentration (% (v/v))	[D2EHPA]	5–30
	Stirring speed (rpm)	SS	100–1,200

the internal phase (V_{int}). The volume (V_s) is calculated by the mass balance.

$$V_s = V_{ext}\frac{10^{-\mathrm{pH}_0} - 10^{-\mathrm{pH}}}{10^{-\mathrm{pH}} - C_{H^+}^{int}} \quad (4)$$

where V_{ext} is the initial volume of the external phase, $C_{H^+}^{int}$ is the initial concentration of H^+ in the internal phase, pH_0 is the initial pH of the external phase, and pH corresponds to the pH of the external phase in contact with the emulsion at any time. The breakup was estimated using RBF network and the results were compared to those obtained experimentally.

3.1.1. Training results

The optimum network structure of ANN model and its parameter variation were determined based on an optimization of the spread constant for a given low RMSE. In order to minimize the error, suitable adjustments were made for each of the weights of the network. Fig. 3 depicted the optimization of the spread constant for the RBF network, the optimum value of the spread constant was obtained by maximizing the observed data obtained from the evidence model. It can be seen that the optimum value of the spread constant was 0.5383 with a square mean root error value of 4%.

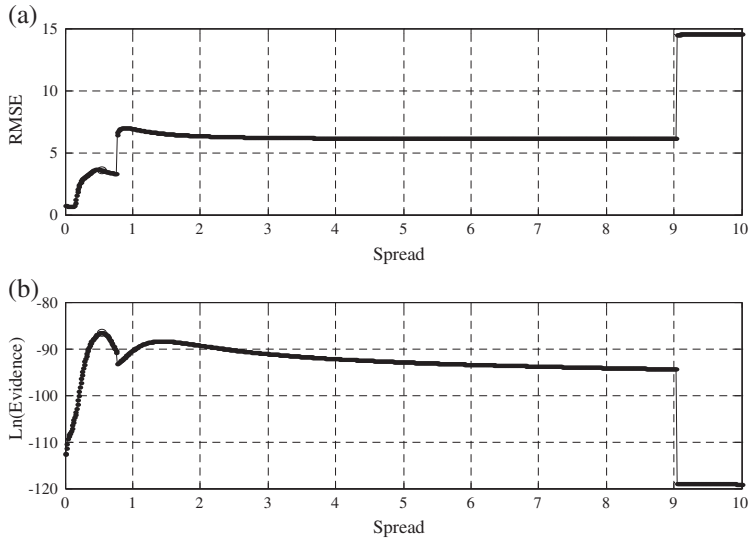

Fig. 3. Optimization of the spread constant of RBF network (a) RMSE vs. spread, (b) Ln (Evidence) vs. spread.

Fig. 4 illustrates the experimental and the predicted emulsion breakage data. The predicted values closely match the experimental data along the diagonal axis with a narrow scatter, which indicates a successful prediction.

3.1.2. Application of emulsion stability model

To examine the effect of the emulsification time on the emulsion stability, the time was varied in the range of 1–10 min. Fig. 5 shows a comparison between the experimental and the predicted emulsion breakage data. Results show that with increase in time of emulsification the breakage percentage decreases up to a certain time but after 3 min, the emulsion stability gradually decreases resulting in increase in breakage percentage. Initially as time elapsed more and more small globules are formed in the system. This results in an increase in the surface area available for mass transfer and increase the emulsion stability. But at the same time, spill of the internal phase might arise as a result of the smaller size of the emulsion droplets. Although the interface area available for mass transfer increases with time, but leakage of the internal stripping phase into the external aqueous phase resulted in the rupture of membrane phase [3]. It can be seen in Fig. 5 that the experimental data and predicted results values obtained from the proposed RBF network were compared and found that the ANN model shows a good performance. An emulsification time of 3 min was selected for further studies in this work.

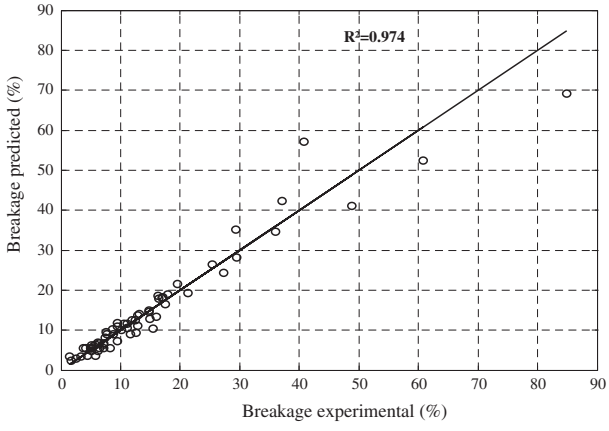

Fig. 4. Comparison between experimental and the predicted emulsion breakage data.

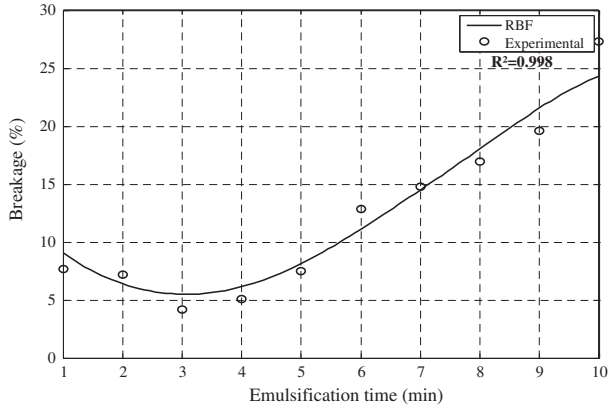

Fig. 5. Effect of emulsification time on the emulsion stability.

The examination of the experimental data and RBF network outputs as a function of the ultrasonic power is described in Fig. 6. The results showed that RBF network modeling could successfully predict the experimental data. Both the experimental data and RBF network prediction demonstrate that the optimum value was 20 W. From Fig. 6, it has been observed that with increase in the ultrasonic power, the breakage percentage decreased up to a certain limit. Initially, a sufficient emulsification occurs with increase in the ultrasonic power. When the ultrasonic power increases the shear force, which acts on the large emulsion droplets, makes the droplets smaller for which the effective interface area available for mass transfer increases. However, increasing the ultrasonic power above a critical value (20 W), the stability of the emulsion reduced significantly with a corresponding increase in the breakage percentage.

Fig. 7 depicted the influence of the stirring speed on the emulsion stability. It has been observed that the breakage percentage increases with increasing the stirring speed. The stirring speed which provides adequate membrane stability and minimum emulsion swelling was 200 rpm. When stirring speed was less than 200 rpm the breakage percentage was low. This may be attributed to the fact that with decreasing the stirring speed, the globules diameter increases and hence the area for mass transfer decreases [3]. Fig. 7 shows a good agreement between the predicted results and the corresponding experimental data.

Fig. 8 presents the effect of sulfuric acid concentration on the emulsion stability. As depicted in Fig. 8, an increase in the sulfuric acid concentration from 0.1 to 0.4 M resulted in a decrease in the breakage percentage. There was no considerable decrease in the breakage percentage when the concentration of sulfuric acid gradually increased beyond 0.4 M. "This may be due to the reaction between sulfuric acid and the surfactant (Span80), which results in a partial loss of the surfactant properties" [2]. According to results shown in Fig. 8, the experimental data were well represented by the RBF network model.

The effect of the extractant concentration on the emulsion stability is shown in Fig. 9. The results indicated that, the membrane stability decreased with increasing the extractant concentration. An excessive increase in the extractant concentration produces some emulsion rupture, present interfacial characteristics that induce failure of internal aqueous solution, as a consequence of the emulsion breakdown. In addition, too high concentration of the extractant leads to an increase in the viscosity of the liquid membrane, which leads to the generation of larger droplets. The best value of the extractant concentration was found to be 20% (v/v) based on the emulsion stability.

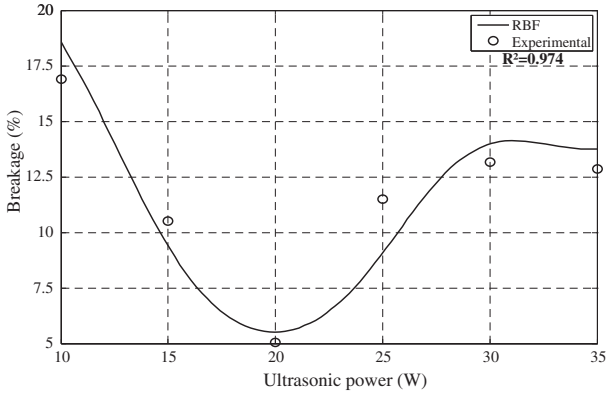

Fig. 6. Effect of ultrasonic power on the emulsion stability.

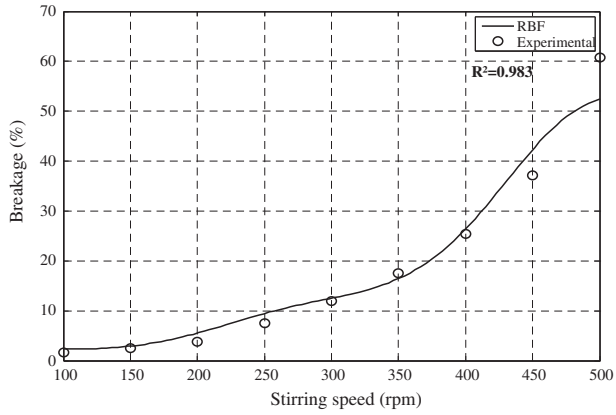

Fig. 7. Effect of stirring speed on the emulsion stability.

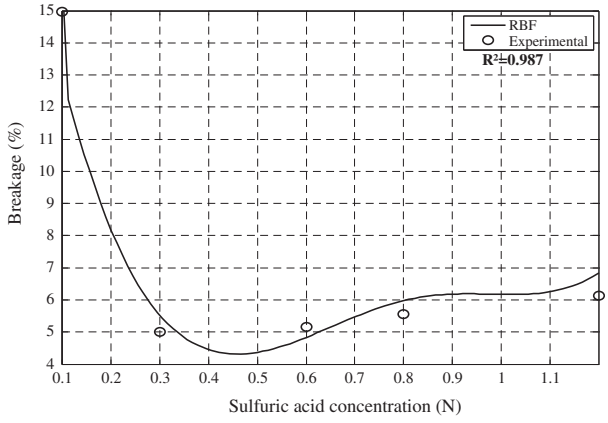

Fig. 8. Effect of sulfuric acid concentration on the emulsion stability.

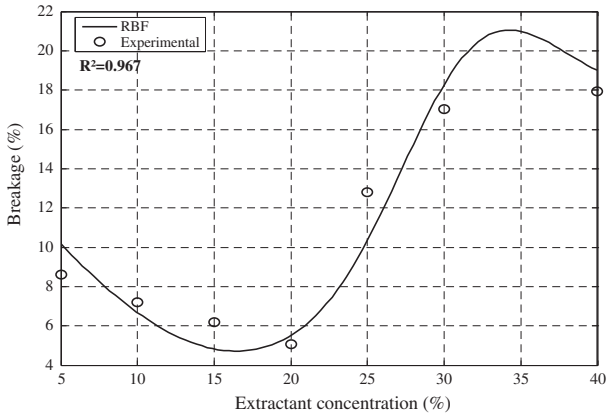

Fig. 9. Effect of extractant concentration on the emulsion stability.

Fig. 9 shows that the results obtained from the proposed RBF network model are in good agreement with the experimental results.

In ELM, the added surfactant was applied as an emulsifier in the liquid membrane phase, which not only affects the stability of the liquid membrane but also the swelling of the emulsion. Fig. 10 shows the effect of the surfactant concentration on the emulsion stability. The comparison of experimental results and RBF network outputs shows that RBF network model prediction was found in a good agreement with the experimental results. For example, the surfactant concentration corresponding to minimum breakage percentage was 4% (v/v) obtained from the experimental results against 4.3% (v/v) obtained from the RBF network.

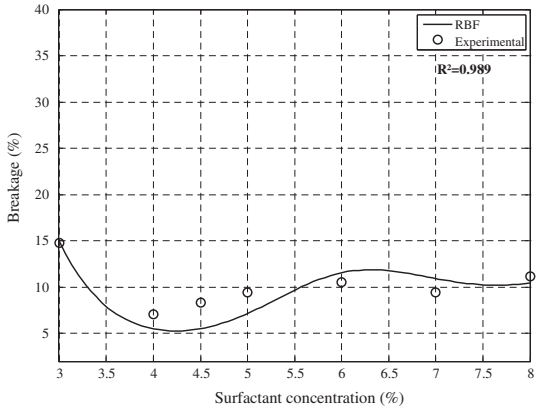

Fig. 10. Effect of surfactant concentration on the emulsion stability.

The effect of the organic phase to the internal phase volume ratio on the emulsion stability was studied (Fig. 11). The volume ratio was varied from 0.5 to 2. Fig. 11 shows that the emulsion stability increases with increasing the volume ratio. This is due to the fact that with increasing volume ratio the number of droplets and the interface surface area available for mass transfer increases. Furthermore, Fig. 11 shows a good agreement between the RBF network model and experimental results. The best value of the organic phase to internal phase volume ratio was taken as 1.

The effect of W/O emulsion to the external aqueous phase volume ratio on emulsion stability was studied. The experiment was done with a different volume ratio of W/O emulsion with aqueous feed phase. The emulsion stability with different W/O emulsion to the external aqueous phase volume ratio is described in

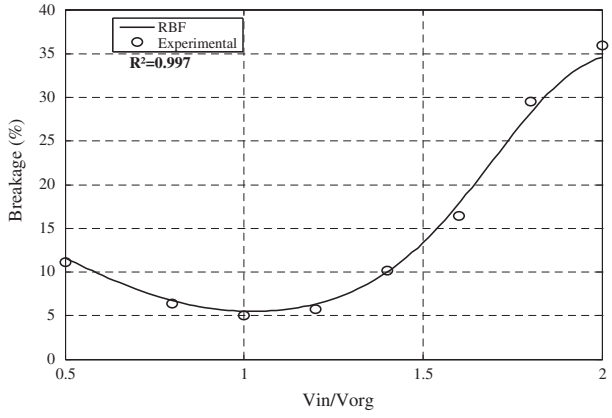

Fig. 11. Effect of the internal phase to organic phase volume ratio on the emulsion stability.

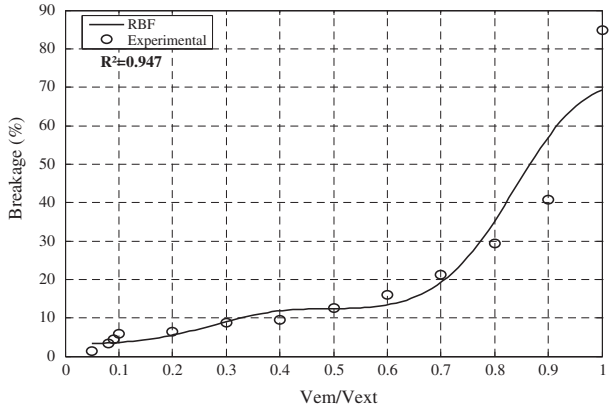

Fig. 12. Effect of the emulsion to the external phase volume ratio on the emulsion stability.

Fig. 12. The breakage percentage increased with increasing the ratio of the emulsion to the external aqueous solution from 0.05 to 1. In addition, the experimental data were well fitted ($R^2 = 0.947$) with the model using RBF network (Fig. 12).

3.2. Removal of copper

3.2.1. Training results

Fig. 13 illustrates the optimization of the spread constant. It can be seen that the optimum value of the spread constant was obtained by maximizing the observed data obtained from the evidence model. The optimum value of the spread constant was 0.6606 with a square mean root error value of 4%.

Fig. 14 illustrates the experimental and predicted breakage percentage data. ANN model predictions were made at optimum spread constant. The predicted values of the breakage percentage were found in match with experimental results.

3.2.2. Application of extraction efficiency model of copper

The effect of the copper concentration on the extraction was studied using different concentrations of copper from 50 to 200 ppm. Fig. 15 shows the experimental results along with the RBF network predicted from the extraction efficiency at different copper concentration. The results show that, the extraction efficiency decreased with increasing the copper concentration. At low copper concentration,

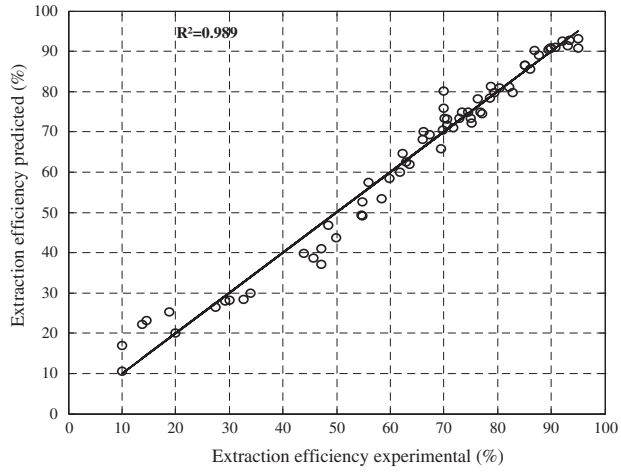

Fig. 14. Comparison between experimental and the predicted extraction efficiency data.

high extraction efficiency was obtained (95%). However, when the copper concentration increased to 200 ppm, the extraction efficiency reached only 74%. These observations may be attributed to the rapid saturation of the copper in the emulsion internal phase. Furthermore, the experimental and the predicted values were in a good agreement. For example, R (50 ppm) = 0.996, R (100 ppm) = 0.995, R (150 ppm) = 0.997, and R (200 ppm) = 0.994.

The effect of stirring speed on the copper extraction efficiency was studied over the range of 200–1,200 rpm. Fig. 16 indicates that the extraction efficiency decreased with increasing stirring speed reaching to an optimal level (200 rpm). Later, an

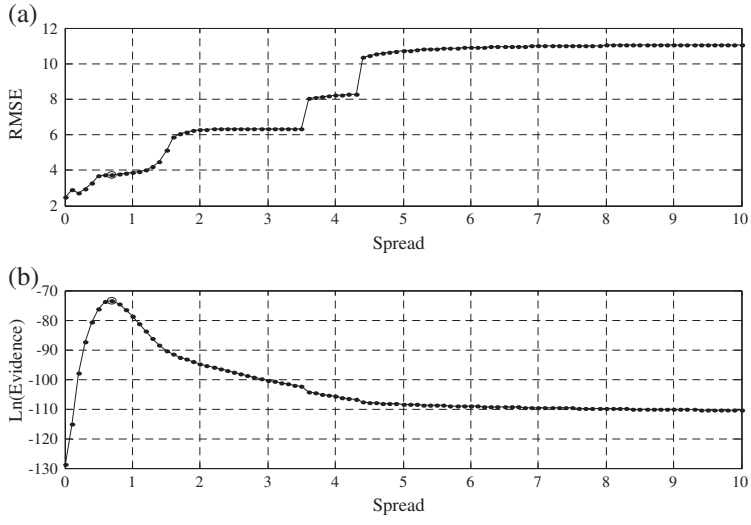

Fig. 13. Optimization of the spread constant of RBF network (a) RMSE vs. spread, (b) Ln (Evidence) vs. spread.

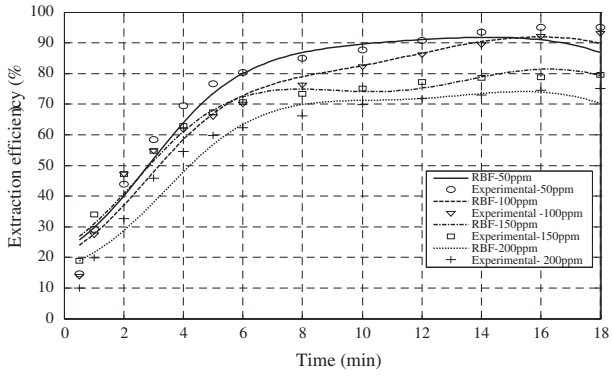

Fig. 15. Effect of the copper concentration in the external phase on the extraction efficiency.

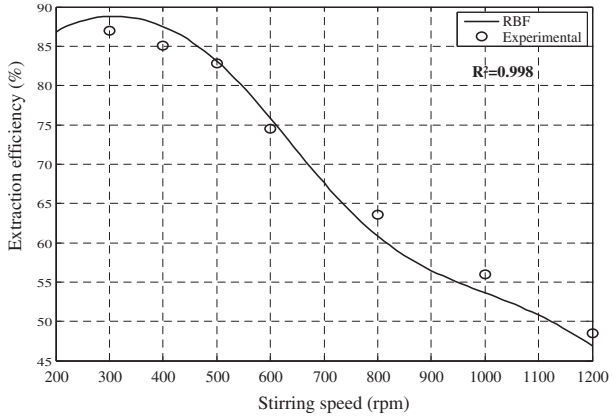

Fig. 16. Effect of the stirring speed on the extraction efficiency.

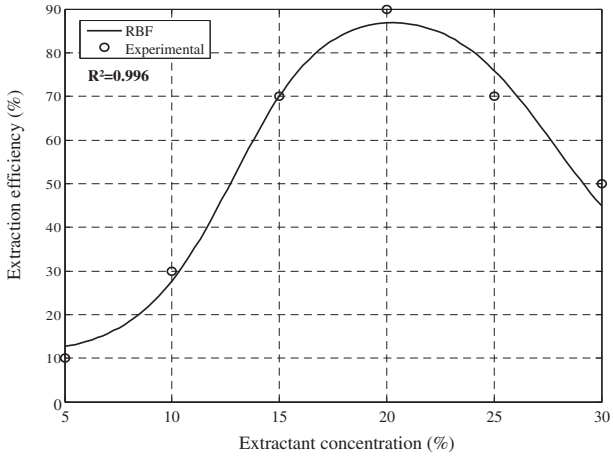

Fig. 17. Effect of the extractant concentration on the extraction efficiency.

increase in stirring speed decreased the extraction efficiency. When the stirring speed increase, the size of the emulsion globules decreased and consequently, the interfacial area available for mass transfer increased. On the other hand, increasing the stirring speed above a critical value, the stability of emulsion decreased considerably as a result of the emulsion breakup, which is induced by leakage from the internal aqueous phase. In the view of the results above, it can be said that the RBF network model provided a good prediction for the experimental results.

The extractant concentration plays a vital role in the overall behavior of the ELM extraction process. Fig. 17 shows the effect of the extractant concentration on the extraction efficiency. The extraction efficiency increased with increase in the extractant concentration (5% (v/v)–20% (v/v)). But after a critical value of the extractant concentration (20% (v/v)) the extraction efficiency decreased significantly. After a critical extractant concentration the degree of emulsion stability decreased due to increase in membrane viscosity. The optimum value of the extractant concentration was found to be 20% (v/v). Similar value for the optimum concentration was predicted from RBF network model. In addition, the experimental results and the predicted values were in a good agreement.

4. Conclusion

The results indicated that the ANN can be used successfully to predict the optimum operational parameters which lead to a good stability of the emulsion and a maximum copper removal. The operational conditions conducting to an excellent stability W/O emulsion were: emulsification time: 3 min; ultrasonic power: 20 W; stirring speed: 200 rpm; sulfuric acid concentration: 0.3 N; extractant concentration: 20% (w/w); concentration of surfactant: 4% (w/w); volume ratio of internal phase to organic phase: 1; and volume ratio of W/O emulsion to external phase: 0.2. The result reveals that there is a good agreement between RBF network model and the experimental values. In addition, the RBF network can be applied as a powerful tool to effectively predict the performance of the ELM process.

Acknowledgments

This work was financially supported by the Ministry of Higher Education and Scientific Research of Algeria (Project No. E01620130023).

References

[1] N.N. Li, Separating hydrocarbons with liquid membranes, US Patent 3 (1968) 410–794.
[2] R. Sabry, A. Hafez, M. Khedr, A. El-Hassanin, Removal of lead by an emulsion liquid membrane, Desalination 212 (2007) 165–175.
[3] M. Chiha, O. Hamdaoui, F. Ahmedchekkat, C. Pétrier, Study on ultrasonically assisted emulsification and recovery of copper(II) from wastewater using an emulsion liquid membrane process, Ultrason. Sonochem. 17 (2010) 318–325.
[4] B. Sengupta, R. Sengupta, N. Subrahmanyam, Copper extraction into emulsion liquid membranes using LIX 984 N-C, Hydrometallurgy 81 (2006) 67–73.
[5] F. Valenzuela, C. Fonseca, C. Basualto, O. Correa, C. Tapia, J. Sapag, Removal of copper ions from a waste mine water by a liquid emulsion membrane method, Miner. Eng. 18 (2005) 33–40.
[6] M. Ludres, F. Gameiro, P. Bento, M. Rosinda, C. Ismael, M. Teressa, A. Reis, J.M.R. Carvalho, Extraction of copper from ammoniacal medium by emulsion liquid membrane using LIX 54, J. Membr. Sci. 293 (2007) 151–160.
[7] Y.T. Mohamed, A.H. Ibrahim, Extraction of copper from waste solution using liquid emulsion membrane, J. Environ. Prot. 3 (2012) 129–134.
[8] A. Kargani, T. Kaghazchi, M. Soleimani, Mathematical modeling of emulsion liquid membrane pertraction of gold (III) from aqueous solution, J. Membr. Sci. 279 (2005) 380–388.
[9] M. Chakraborty, C. Bhattacharya, S. Datta, Study of the stability of W/O/W-type emulsion during the extraction of nickel via emulsion liquid membrane, Sep. Sci. Technol. 39 (2004) 2609–2625.
[10] Y. Park, A.H.P. Skelland, L.J. Forney, J.H. Kim, Removal of phenol and substituted phenols by newly developed emulsion liquid membrane process, Water Res. 40 (2006) 1763–1772.
[11] P. Gandhidasan, M.A. Mohandes, Predictions of vapor pressures of aqueous desiccants for cooling applications by using artificial neural networks, Appl. Therm. Eng. 28 (2008) 126–135.
[12] N. Messikh, M.H. Samar, L. Messikh, Neural network analysis of liquid–liquid extraction of phenol from wastewater using TBP solvent, Desalination 208 (2007) 42–48.
[13] M. Chakraborty, C. Bhattacharya, S. Dutta, Studies on the applicability of artificial neural network (ANN) in emulsion liquid membranes, J. Membr. Sci. 220 (2003) 155–164.
[14] B. Karaağaç, M. İnal, V. Deniz, Artificial neural network approach for predicting optimum cure time of rubber compounds, Mater. Des. 30 (2009) 1685–1690.
[15] A. Schwartz, Prediction of rheometric properties of compounds by using artificial neural networks, R. Chem. Technol. 74 (2001) 16–23.
[16] C. Deshmukh, J. Senthilnath, M. Dixit, N. Malik, A. Pandey, N. Vaidye, N. Omkar, N. Mudliar, Comparison of radial basis function neural network and response surface methodology for predicting performance of biofilter treating toluene, J. Soft. Eng. Appl. 5 (2012) 595–603.
[17] H. Liu, Y. Wen, F. Luan, Y. Gao, Application of experimental design and radial basis function neural network to the separation and determination of active components in traditional Chinese medicines by capillary electrophoresis, Anal. Chim. Acta 638 (2009) 88–93.
[18] Y. Liu, Q. Zheng, Z. Shi, J. Chen, Training radial basis function networks with particle swarms, Lect. Note. Comp. Sci. 3173 (2004) 317–322.